Developmental order, fibre caliber, and vascularization predict tract-wise declines: Testing retrogenesis and physiological predictions in white matter aging

Tyler D. Robinson[1], Jordan A. Chad[1], Yutong L. Sun[1], Paul T. H. Chang[1], J. Jean Chen[1,2,3]

1. Rotman Research Institute, Baycrest, Canada
2. Medical Biophysics, University of Toronto, Canada
3. Biomedical Engineering, University of Toronto, Canada

Corresponding authors:
J. Jean Chen (jchen@research.baycrest.org)
Tyler D. Robinson (trobinson@research.baycrest.org)

Rotman Research Institute, Baycrest
3560 Bathurst Street
Toronto ON, Canada M6A 2E1

ABSTRACT

To understand the consistently observed spatial distribution of white-matter (WM) aging, developmentally driven theories of retrogenesis have gained traction, positing that the order WM development predicts declines. Regions that develop first are often expected to deteriorate the last, i.e. “last-in-first-out”. Alternatively, regions which develop most rapidly may also decline most rapidly in aging, or the “gains-predict-loss” model. The validity of such theories remains uncertain, in part due to lack of clarity on the definition of developmental order. Our recent findings also suggest that WM degeneration may vary by physiological parameters such as perfusion. Furthermore, it is informative to link perfusion to fibre metabolic need, which varies with fibre size. Here we address the question of whether WM degeneration is determined by development trajectory or physiological state across both microstructural and perfusion measures using data drawn from the Human Connectome Project in Aging (HCP-A). Our results indicate that developmental order of tract myelination provides the strongest support for the retrogenesis hypothesis, with the last to complete myelination the first to decline. Moreover, higher mean axon diameter and lower macrovascular density are associated with lower degrees of WM degeneration across measures. Tract perfusion, in turn also tends to be higher and the arterial transit time longer for tracts that appear first. These findings suggest that WM degeneration in different tracts may be governed by their developmental trajectories and physiology, and ultimately influenced by each tract’s metabolic demand.

Keywords: White Matter, Aging, Retrogenesis, Diffusion, Perfusion, Microstructure

INTRODUCTION

There are well-documented spatial variations in the distribution of WM microstructural aging (Cox et al., 2016; de Groot et al., 2016; Michielse et al., 2010; Schilling et al., 2022; Slater et al., 2019), however, attempts to model the mechanism of these differences across the brain have produced only mixed success (Kiely et al., 2022; Slater et al., 2019; Yeatman et al., 2014). Developmentally driven models of brain aging pose an inverse relationship between tract-wise white matter (WM) development and later declines in aging. These retrogenesis theories have gained considerable traction, positing that order or trajectory of tract-wise white matter (WM) development predicts later declines, sometimes simplified to suggest that degeneration occurs first in anterior, and last in posterior regions (Hoagey et al., 2019), i.e. "last-in-first-out (LIFO)". However, the validity of LIFO theories remains uncertain in microstructural research, in part due to lack of clarity in defining first or last "in" in the context of numerous measures of neural development. In fact, irrespective of which tract is first to appear, many regions of the brain continue to mature into adulthood (Lebel & Beaulieu, 2011; Yeatman et al., 2014). An alternative theory, termed "gain-predicts-loss" (Slater et al., 2019), posits that the rate of development predicts the rate of later declines, in which those regions which develop most rapidly will also decline most rapidly in aging. However, there are again several metrics by which the rate of development can be asserted (Grotheer et al., 2022; H. Huang et al., 2006; Kiely et al., 2022; Yu et al., 2020).

While existing research has focused largely on microstructural measures of WM integrity (Slater et al., 2019), microvascular measures of WM declines have remained an underrepresented area of research on WM aging, due in part to the previous difficulty of imaging perfusion in the WM directly (Bernbaum et al., 2015; Chen et al., 2013). The importance of neurovascular health in maintaining tissue integrity in aging is increasingly recognized, as associations have been observed between cortical perfusion and the development of WM lesions (Chen et al., 2013), as well as between WM perfusion and microstructural integrity in the aging WM directly (Robinson et al., 2023). As a result, growing evidence of regional differences in white matter (WM) perfusion is poised to join established literature on WM differences in aging trajectories.

One of the earliest markers available for defining a tract as "in" in the context of a developmentally ordered last-in-first-out model is the point at which a tract becomes recognizable in prenatal development (H. Huang et al., 2009; Ouyang et al., 2021). Prior to the emergence of a tract as a distinct structure in the prenatal brain, meaningfully differentiating regions for comparison to adult tracts becomes conceptually challenging. As one of the earliest possible ways to define a tract's arrival, prenatal emergence thus represents a valuable starting point for examining retrogenesis predictions. The degree to which this stage of development can be considered a foil for WM degeneration in aging remains unclear,

as the earliest stages of tract development may have less in common with age-related degeneration than later and ongoing developmental processes such as myelination, though the earliest stages of axonal myelination similarly take place prenatally (Brody et al., 1987; Grotheer et al., 2022). While the process of myelination continues into adulthood (Arshad et al., 2016; Slater et al., 2019; Stricker et al., 2009), the degree of myelination at birth as defined by R1 values may represent a proxy measure for developmental state in the context of retrogenesis under the assumption that those tracts showing highest myelin density at birth are those which begin myelinating earliest (Grotheer et al., 2022).

While last-in-first-out models of retrogenesis can be addressed via early WM developmental states, addressing gain-predicts-loss hypotheses into adulthood requires incorporating ongoing rates of WM maturation. Peak microstructural integrity across the lifespan has been posited as a measure of the full maturation of a region (Slater et al., 2019; Yu et al., 2020). However, tract-wise ages of peak mean diffusivity (MD) do not mirror the order in which tracts reach peak R1 values indicating maturation of axonal myelination (Yeatman et al., 2014), necessitating separate predictive models. Notably, myelination state at birth and rates of myelination into adulthood also demonstrate differing orders by tract (Grotheer et al., 2022; Slater et al., 2019).

In addition to early developmental orders and rates of tract maturating, physiological determinants such as axon diameter have been considered a measure of WM maturation, as increasing axon diameter is a notable component of early WM fiber development and associated with function (Genc et al., 2018; S. Y. Huang et al., 2020). Our recent findings suggest that WM degeneration may also vary by both axonal diameter and perfusion (Robinson et al., 2023). As a result, incorporating physiological differences between tracts can be considered both a component of, and a complement to, developmental retrogenesis models. For the purposes of this study, we have targeted mean axonal diameter and macrovascular density as relevant physiological determinants for tract-wise differences in WM aging.

The degree to which WM degeneration in aging is determined by development trajectory or physiological factors is central to understanding the mechanisms of WM degeneration. Using diffusion MRI (dMRI) and perfusion data drawn from the Human Connectome Project in Aging (HCP-A) data set, this study aims to test tract-wise retrogenesis predictions in WM integrity across six models of WM development and maturation drawn from existing literature to determine which, if any, best represent degrees and rates of decline in the aging WM. We hypothesized that one or more models will show support for the retrogenesis hypothesis, such that earliest developing tracts will exhibit the most advanced declines in aging. Given existing support for the last-in-first-out hypothesis, we further hypothesized that the last-in-first-out model of myelination state based ordering would demonstrate the best fit model. Additionally, in light of prior research demonstrating associations between microstructural integrity and perfusion in the aging WM, we secondarily hypothesized that the macro-vascular density model would

also be significantly associated with age-related WM declines in either microstructural or perfusion measures.

METHODS

535 healthy adult subjects (300 female, aged 36-100, aprox. 48% postmenopausal) were drawn from the HCP-A dataset (OMB Control# 0925-0667) (Bookheimer et al., 2019; Harms et al., 2018). All subjects were assessed to be in good health and without pathological cognitive impairment (i.e. stroke, clinical dementia). Manual quality control identified thirty-two subjects for exclusion from the original sample due to MRI artifacts that produced notable errors when generating WM masks. Three additional subjects were excluded as age outliers due to being the only subjects of 100 years of age, bringing the final sample size to 500 subjects (249 female, aged 36-89) (**Table 1**).

Table 1: Sample Demographics
Demographic statistics for all subjects, female subjects, and male subjects. All subjects were in good health and without pathological cognitive impairment (i.e. stroke, clinical dementia)

	Count	Mean Age (years)	Median Age (Years)	Age Range (Years)	Age Stdev (Years)	Hypertension Count	Education (years)
All	**500**	**57.88**	**56**	**36-89**	**14.3**	**133**	**17.41**
Female	294	57.27	54	36-89	14.4	63	17.29
Male	206	58.76	58	36-89	14.2	70	17.58

The study accessed T1-weighted structural MRI, diffusion-weighted MRI (dMRI), with a 1.5mm^3 voxel resolution, MB=4, with 93 directions at b=1500s/mm^2), and multi-delay multi-band echo planar imaging (MB-EPI) pseudo-continuous arterial spin labeling (pCASL) with a 2.5mm^3 voxel resolution, MB=6, with TIs = 0.7, 1.2, 1.7, 2.2, and 2.7. Data were collected using four matched Siemens Prisma 3T MRI scanners. Further imaging parameters for structural, diffusion, and perfusion imaging can be found in (Harms et al., 2018).

Image analysis

dMRI data were corrected for eddy-current and susceptibility-related distortions via EDDY, and eighteen major WM tracts were reconstructed from the dMRI data using FreeSurfer TRACULA (v 7.2.0) (Maffei et al., 2021; Yendiki et al., 2011), then combined bilaterally to produce ten tracts of interest for

analysis in local space using FSL's fslmaths function. Resulting bilateral tracts included the major forceps (Fmajor), minor forceps (Fminor), anterior thalamic radiation (ATR), cingulum angular bundle (CAB), cingulate gyrus (CCG), corticospinal tract (CST), inferior longitudinal fasciculus (ILF), superior longitudinal fasciculus parietal (SLFP), superior longitudinal fasciculus temporal (SLFT), and the uncinate fasciculus (UNC) (**Figure 1**). This choice of tract segmentations was made to minimize spatial overlap between tracts.

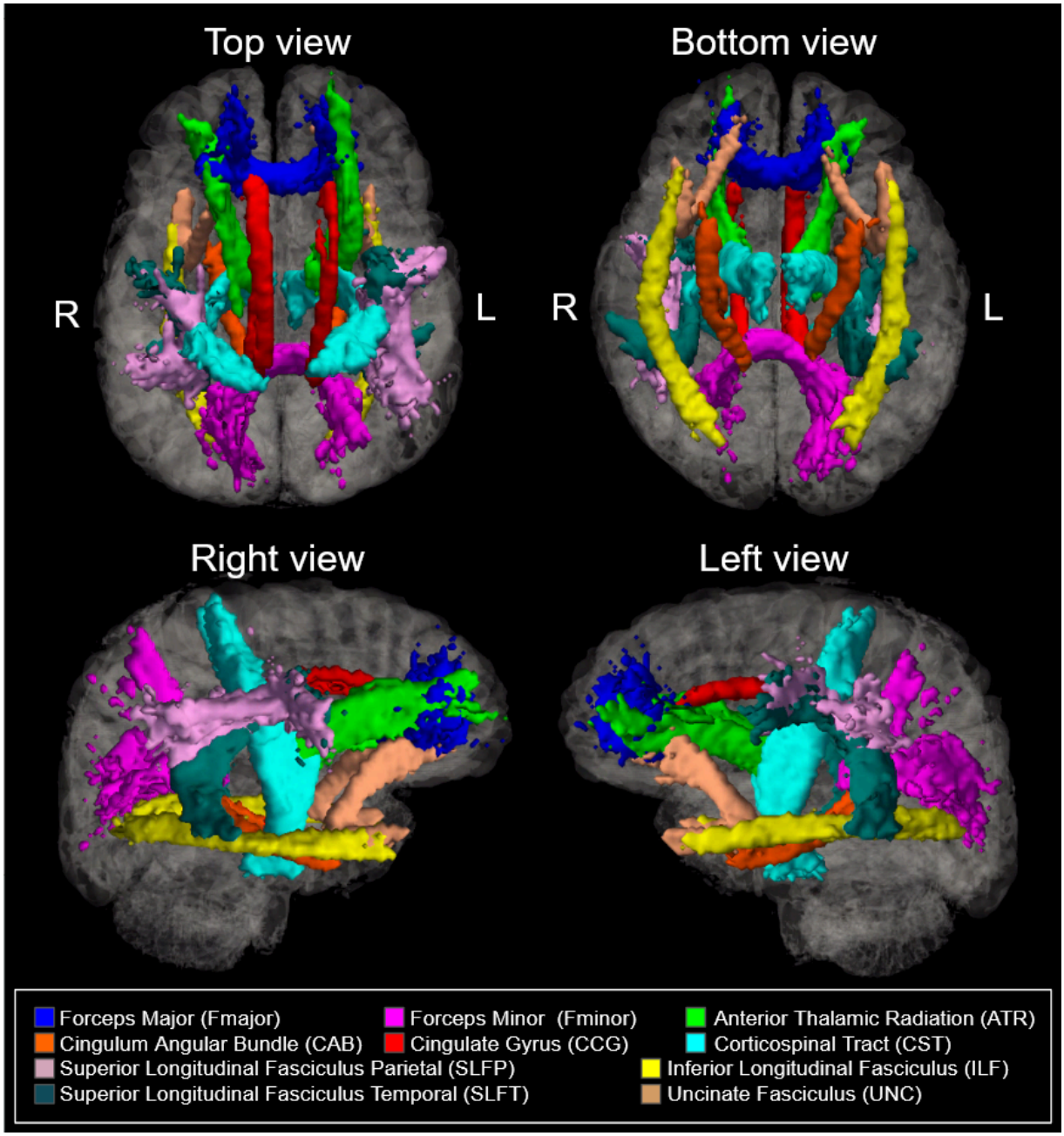

***Figure 1**: Ten bilateral tracts of interest reconstructed using Freesurfer's TRACULA package. This collection of tracts of interest was selected to limit overlap between tracts of interest.*

Microstructure

Microstructural integrity in WW tracts was quantified using fractional anisotropy (FA), mean diffusivity (MD), axial diffusivity (AD), and radial diffusivity (AD) measures. FA, MD, AD, and RD maps were derived via Dipy's DKI script to achieve kurtosis-corrected DTI metric fitting due to the high b-value used in the HCP-A acquisitions. Per-subject tract masks generated by TRACULA were applied to local dMRI images in flsmaths to generate tract means for FA, MD, AD, and RD respectively. For each metric, baseline normalized (percent of baseline) values were calculated as individual raw tract values divided by the mean raw tract value of the youngest 10% of subjects to assess percent differences from the youngest baseline, resulting in "FA_{perc}", "MD_{perc}", "AD_{perc}", "RD_{perc}" values used in subsequent analyses.

Perfusion

Cerebral blood flow (CBF) was quantified using the general kinetic model that accounts for arterial-transit delay (ATT) (FSL oxford_ASL) (Chappell et al., 2009, 2011) to produce per-subject maps of both CBF and ATT in local space. As with microstructural measures, TRACULA-generated tract masks were applied to the local maps using fslmaths to produce tract means for raw CBF AND ATT. Baseline normalized perfusion values were again calculated as individual raw tract values divided by the mean raw tract value of the youngest 10% of subjects (i.e. the baseline group) to produce "CBF_{perc}" and "ATT_{perc}" measures for use in subsequent analyses.

Statistical analysis

Relationships between model order, age, and tract-wise measures of mean WM microstructure and perfusion were assessed using multivariate regression in R (version 4.1.1). Tract-wise age effects were assessed using linear regression of age onto FA_{perc}, MD_{perc}, CBF_{perc}, and ATT_{perc}. Rosner's tests were performed to identify and exclude volume outliers per tract in single tract analyses. The resulting subject counts for these analyses were: Fmajor (N=493), Fminor (N=493), ATR (N=497), CAB (N=490), CCG (N=495), CST (N=491), ILF (N=497), SLFP (N=497), SLFT (N=495), and UNC (N=495). Retrogenesis predictions for mean tract values across ages were assessed via linear regression of tract order onto microstructural and perfusion measures with sex as a regressor of no interest. Tract-wise differences in age effects were assessed via linear regression of tract order, age, and the interaction effect by tract order on age onto microstructure and perfusion measures with sex as a regressor of no interest. Tract orders used in each analysis were determined using six ordered models drawn from existing literature:
Last-in-first-out models;

(1) "Last-appearing-first-out" (LAFO): ordered by time of prenatal emergence (Ouyang et al., 2021). The order variable comprises the ATR, CCG, CST, Fminor, UNC, CAB, ILF, Fmajor, and SLF (combined SLFP/SLFT) in order of earliest to latest prenatal emergence.

(2) "Last-myelinated-first-out" (LMFO): ordered by R1 ("myelination") at birth (Grotheer et al., 2022). The order variable comprises the CST, ATRL, SLF (combined SLFP/SLFT), UNC, ILF, Fmajor, CCG, and Fminor in order of lowest to highest degree of myelination at birth.

Gain-predicts-loss models;

(3) "Slowest-peak-first-out" (SPFO-MD): ordered by rate of MD change from adolescence to adult peak (Slater et al., 2019). The order variable comprises the Fmajor, Fminor, SLF (combined SLFP/SLFT), CST, CCG, ATR, ILF, and UNC in order or lowest to highest rate of MD change.

(4) "Slowest-myelinated-first-out (SMFO): ordered by rate of R1 change from adolescence to adult peak (Slater et al., 2019). The order variable comprises the SLF (combined SLFP/SLFT), Fmajor, Fminor, CST, CCG, ILF, ATR, and UNC in order of lowest to highest rate of myelination.

Physiological determinant models:

(5) "Axon-diameter-determined" (ADD): ordered by mean axon diameter at birth (S. Y. Huang et al., 2020). The order variable comprises the UNC, Fminor, ILF, CAB, ATR, CCG, SLFT, SLFP, Fmajor, and CST in order of lowest to highest mean axon diameter at birth.

(6) "Vascular-diameter-determined" (VDD): ordered by mean macrovascular density (Bernier et al., 2020). The order variable comprises the SLF (combined SLFP/SLFT), CST, Fmajor, UNC, ILF, and Fminor in order of lowest to highest mean macrovascular density.

Tracts were ordered under each of these models, as specified in **Table 2**. Additionally, tract-wise linear regressions in terms of both the tract "state" and "rate" values. That is, under the tract ordering in each of these models, we assessed the association between the tract rank and the mean tract parameters ("state-based") as well as the association with the regression coefficient against age ("rate-based"), with sex as a covariate of no interest. Tract parameters include both microstructural (FA_{perc}, MD_{perc}) and perfusion (CBF_{perc}, ATT_{perc}) measures.

Table 2: Model definitions and corresponding tract order directionalities

Model	**Tract order**	
	Low	**High**
LAFO (last appearing first out)	First appearing	Last appearing

LMFO (last myelinating first out)	First myelinating	Last myelinating
SPFO-MD (slowest peaking first out)	Lowest rate of MD change from adolescence to adult peak	Highest rate of MD change from adolescence to adult peak
SMFO (slowest myelinating first out)	Lowest rate of R1 change from adolescence to adult peak	Highest rate of R1 change from adolescence to adult peak
ADD (axon diameter determined)	Lowest axon diameter	Highest axon diameter
VDD (vascular density determined)	Lowest macrovascular density	Highest macrovascular density

Effects of sex

Sex differences in the effects of model order on mean microstructural (FA_{perc}, MD_{perc}, AD_{perc}, RD_{perc}) and perfusion (CBF_{perc}, ATT_{perc}) measures were conducted per ordered model using using multivariate regression of tract order, sex, and the interaction effect of sex by tract order onto each respective microstructural/perfusion measure. Similarly, sex differences in the effects of model order on rates of microstructural (FA_{perc}, MD_{perc}, AD_{perc}, RD_{perc}) and perfusion (CBF_{perc}, ATT_{perc}) declines per ordered model with age were assessed via multivariate regression of tract order, age, sex, the interaction of tract order by sex, and the three-way interaction of tract order, age, and sex onto each respective microstructural/perfusion measure.

RESULTS

Age-related declines were observed in MD_{perc} for all ten tracts, and in FA_{perc} for seven of ten tracts (Fmajor, Fminor, ATR, CAB, CCG, ILF, and SLFP). Eight of ten tracts (Fmajor, ATR, CAB, CST, ILF, SLFP, SLFT, UNC) demonstrated significant age-related increases in AD_{perc}, while significant declines in AD_{perc} were identified in the CCG alone. All ten tracts showed significant age-related increases in RD_{perc}. Age-related declines in CBF_{perc} were identified in eight of ten tracts (Fmajor, ATR, CAB, CCG, CST, ILF, SLFP, SLFT, and UNC), along with age-related increases in ATT_{perc} in seven of ten tracts (Fminor, ATR, CCG, CST, SLFP, SLFT, and UNC) (**Figure 2**).

Order of state of microstructure declines

Last-in-first-out models

Both last-in-first-out models demonstrated significant associations with at least one measure of microstructural integrity, with the LAFO model showing greater declines in earlier appearing tracts and the LMFO model showing greater declines in those which myelinate latest. In the LAFO model, tract development order was positively associated with mean FA_{perc} alone, while no significant association with MD_{perc} was observed. AD_{perc} was found to be positively associated with tract emergence order, however, no significant association was identified with RD_{perc}. In LMFO, FA_{perc} was found to be inversely related to R1 order, while MD_{perc} was positively associated with tract order. Examination of AD_{perc} and RD_{perc} values revealed significant associations between both and the order variable, such that AD_{perc} was negatively associated with myelination order while RD_{perc} was positively associated (**Figure 3a**).

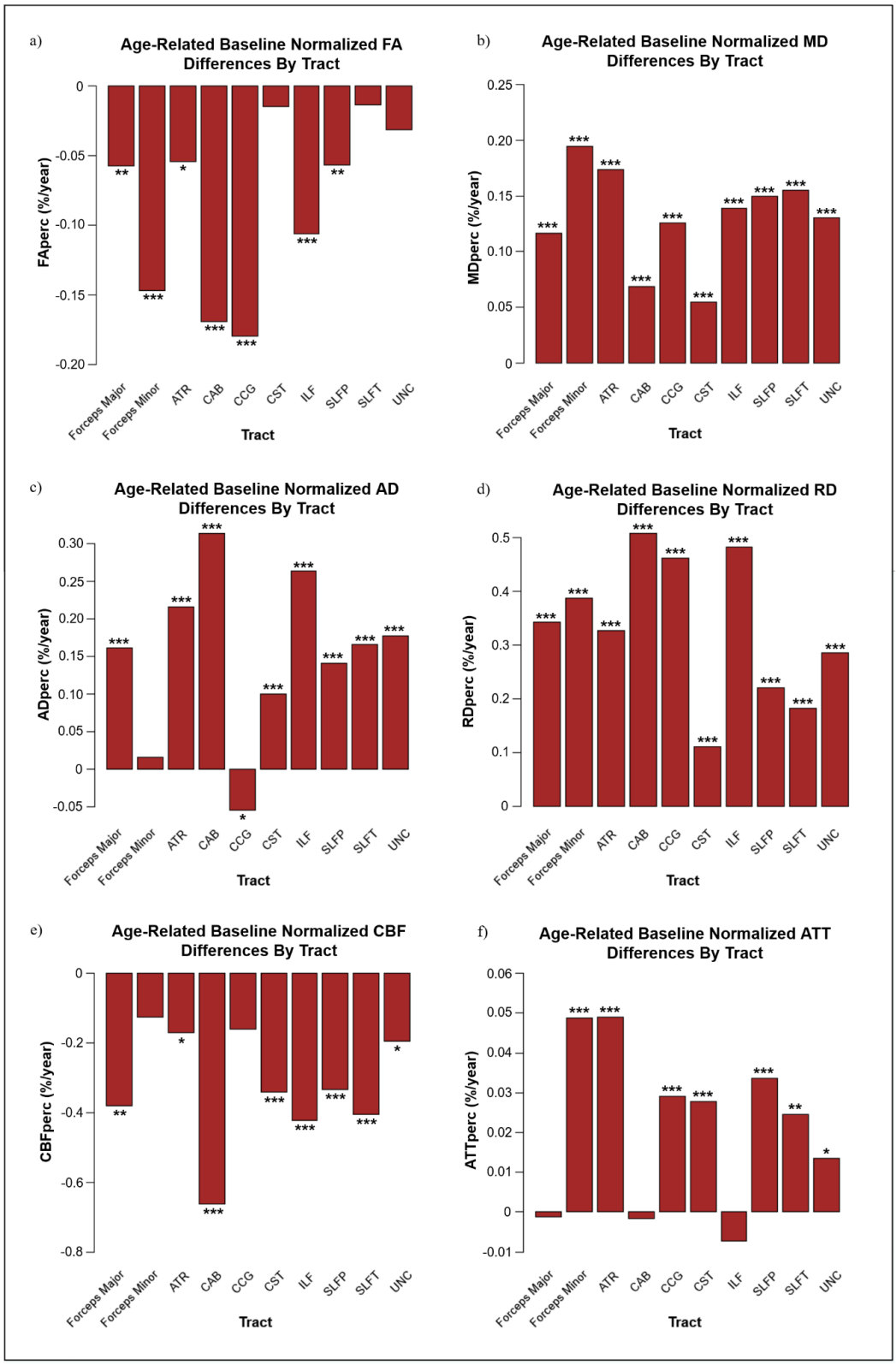

Figure 2: *Tractwise age effects for FA_{perc} (a), MD_{perc} (b), AD_{perc} (c), RD_{perc} (d), CBF_{perc} (e), and ATT_{perc} (f) respectively. Significant effects by sex and age are denoted with asterisks (***: p<.001, **: p<.01, and *: p<.05).*

Gain-predicts-loss models

Regarding gains-predicts-loss predictions, AD_{perc} and RD_{perc} demonstrated the only significant associations in either mean microstructural measures or rate-of-decline interactions, with both AD_{perc} and RD_{perc} associating positively with rate of myelination under the SMFO model as faster myelinating tracts demonstrated the highest microstructural effects. No significant associations were identified by FA_{perc} or MD_{perc} in the SMFO model in either mean microstructural measures, and no significant associations were identified for any microstructural variables in either mean microstructural under the SPFO-MD model (**Figure 3b**).

Physiological determinant models

Both physiological determinant models demonstrated significant associations with both FA_{perc} and MD_{perc}. In ADD, a positive association was identified between FA_{perc} and axon diameter such that tracts with higher mean diameter exhibited the highest FA_{perc}, while in VDD, FA_{perc} was found to be negatively related to macro-vascular density order, such that higher macrovascular density was associated with lower FA_{perc}. In contrast, MD_{perc} was positively associated with tract order in the VDD models and negatively associated in the ADD model, complementing patterns identified in FA_{perc}. Examination of AD and RD separately revealed a negative association between AD_{perc} and axon diameter and positive association between RD_{perc} and axon diameter under the ADD model. Conversely, only RD_{perc} demonstrated a significant association under the VDD model, with RD_{perc} associating positively with macrovascular density (**Figure 3c**).

Order of rates of microstructural decline

Last-in-first-out models

In **Figure 4**, for each of the 6 models of tract ordering, we summarize the linear fits of each tract microstructural parameter against age in the colour maps. Bright colours represent higher values in the linearly modeled microstructural parameter, and the regression coefficient against age for different tracts are aggregated and fit against tract rankings. The result allows us to assess the influence of tract ranking under each model on the rate of age-related tract decline. Significant regressions (with sex as a covariate) are indicated by red dashed lines.

In the LAFO model, rate-of-decline analyses revealed a significant interaction between tract emergence order and age effects on AD_{perc} alone. In the LMFO model, tract order demonstrated a negative relationship with age effects on FA_{perc} with a positive interaction between LMFO tract order and age effects on MD_{perc}, such that earliest myelinating tracts were associated with slower microstructural deterioration. AD_{perc} and RD_{perc} comparisons demonstrated a similar pattern of effects in rate-of-decline

interactions to those identified in simple associations, with myelination order interacting positively with age effects on AD_{perc} and negatively with age effects on RD_{perc} (**Figures 4a**).

Gain-predicts-loss models

Tract order in the SMFO model interacted positively with age effects in both AD_{perc} and RD_{perc} in rate-of-decline analyses, i.e. faster myelinating tracts demonstrated the highest rates of microstructural decline with age. No significant interactions were identified by FA_{perc} or MD_{perc} under the SMFO model in rates of decline, and no significant interactions were identified for any microstructural variables in rate-of-decline analyses under the SPFO-MD model (**Figures 4b**).

Physiological determinant models

In rate-of-decline comparisons, in both ADD and VDD models, significant interactions by tract order on association between FA_{perc} and age were observed. In ADD, tract order demonstrated a positive relationship with age effects on FA_{perc}, such that higher axon diameter was associated with slower declines in aging, while in VDD, this relationship was negative as higher vascular density was associated with faster aging declines. Inverse relationships were again observed in the interaction between tract order and age effects on MD_{perc}, with a negative relationship identified in ADD, along with a positive relationship in VDD. Examining AD_{perc} and RD_{perc} separately showed a similar pattern in rate-of-decline analyses to those found in mean microstructural analyses, with axon diameter order interactively negatively with age effects on AD_{perc} and positively with age effects in RD_{perc} under the ADD model, while macrovascular density under the VDD model interacted positively with RD_{perc} alone (**Figures 4c**).

Order of state of perfusion declines

Last-in-first-out models

Both last-in-first-out models identified linear relationships between mean CBF_{perc}/ATT_{perc} and order of early prenatal tract emergence (LAFO) and RI at birth (LMFO) respectively. In the LAFO model, tract order was negatively associated with both CBF_{perc} and ATT_{perc}, i.e. the later emerging tracts had both lower CBF_{perc} and and shorter ATT_{perc} later in life. In the LMFO model, CBF_{perc} associated positively with tract order while ATT_{perc} associated negatively, suggesting tracts last to fully myelinate have higher CBF_{perc} and shorter ATT_{perc} (**Figures 3a**).

Gain-predicts-loss/Physiological determinant models

No significant associations between tract order and mean CBF_{perc}/ATT_{perc} identified by the gain-predicts-loss models (SPFO-MD, SMFO), or the physiological determinant models (ADD, VDD) (**Figures 3b-c**).

Order of rates of perfusion decline

Last-in-first-out models

In the LAFO model alone, the rate of decline analyses identified significant negative associations between tract order and the age associations with $CBF_{perc}/ATT_{perc,}$ such that later emerging tracts exhibit faster decreases in CBF_{perc} but relatively preserved ATT_{perc}. No interaction between tract-order and age-related CBF_{perc}/ATT_{perc} differences was observed in the LMFO model (**Figure 4a**).

Gain-predicts-loss/Physiological determinant models

No significant interactions between tract order and age effects on CBFperc/ATTperc were identified by the gain-predicts-loss models (SPFO-MD, SMFO), or the physiological determinant models (ADD, VDD) (**Figure 4b-c**).

Microstructure-perfusions associations

Seven of ten tracts (Fminor, ATR, CAB, CCG, ILF, SLFP, SLFT) demonstrated significant associations between WM microstructure and WM perfusion on one or more measures. CBF_{perc} was significantly associated with MD_{perc} in the ILF and SLFT, and with FA_{perc} in the CCG. ATT_{perc} was significantly associated with MD_{perc} in the Fminor, ATR, CCG, SLFP, and SLFT, and with FA_{perc} in the ATR and CAB (**Table 3**).

Effects of sex

Examining the effects of sex on microstructural measures in each of the six tested models identified significant interactions with sex in the association between tract order and microstructural state in four of six models. Female subjects demonstrated stronger associations between tract order and mean FA_{perc} than male subjects under the LAFO models, and between tract order and both FA_{perc} and RD_{perc} under the ADD model. Conversely, male subjects demonstrated stronger associations between tract order and mean RD_{perc} than female subjects under the SMFO and VDD models.

In perfusion state analyses, female subjects showed significantly stronger associations between tract order and ATT_{perc} than male subjects under both physiological models (ADD, VDD), while male subjects showed stronger associations between tract order and ATT_{perc} than female subjects under the LMFO model alone (**Table 4a**).

No significant interactions were found between subject sex and the effect of tract order on rates of decline in aging for either microstructural or perfusion analyses under any ordered model (**Table 4b**).

Table 3: Tractwise MD/FA associations with perfusion (covaried for Sex).
All models are multivariate linear regressions based on baseline-normalized measures (x_{perc}) with overall F-statistics, *p*-values, and effect sizes ($R^2_{adjusted}$) listed. Slopes are noted below each regression equation and significant associations bolded with asterisks indicating significance.
(*:p<.05, **:p<.01, ***:p<.001).

	MD_{perc}		**FA_{perc}**	
Tract	CBF_{perc}	ATT_{perc}	CBF_{perc}	ATT_{perc}
Fmajor	$F(2, 490) = 7.47$, $p < .001$, $R^2_{Adjusted} = .03$	$F(2, 490) = 5.68$, $p = .004$, $R^2_{Adjusted} = .02$	$F(2, 490) = 8.24$, $p < .001$, $R^2_{Adjusted} = .03$	$F(2, 490) = 8.08$, $p < .001$, $R^2_{Adjusted} = .03$
	-0.009599	0.081493	-0.003605	-0.010087
Fminor	$F(2, 490) = 1.52$, $p = .22$, $R^2_{Adjusted} = .002$	$F(2, 490) = 6,48$, $p = .002$, $R^2_{Adjusted} = .02$	$F(2, 490) = 5.49$, $p = .004$, $R^2_{Adjusted} = .02$	$F(2, 490) = 5.53$, $p = .004$, $R^2_{Adjusted} = .02$
	-0.011735	**0.289540****	0.019804	-0.227797
ATR	$F(2, 494) = 2.08$, $p = .13$, $R^2_{Adjusted} = .004$	$F(2, 494) = 9.13$, $p < .001$, $R^2_{Adjusted} = .03$	$F(2, 494) = 3.23$, $p = .009$, $R^2_{Adjusted} = .04$	$F(2, 494) = 4.22$, $p = .015$, $R^2_{Adjusted} = .01$
	-0.014611	**0.324941*****	0.027963	**-0.306558****
CAB	$F(2, 487) = 0.47$, $p = .62$, $R^2_{Adjusted} = -.002$	$F(2, 487) = 2.69$, $p = .07$, $R^2_{Adjusted} = .007$	$F(2, 487) = 0.75$, $p = .47$, $R^2_{Adjusted} = -.001$	$F(2, 487) = 4.53$, $p = .01$, $R^2_{Adjusted} = .01$
	0.0006211	-0.202510	0.01026	**0.79903***
CCG	$F(2, 492) = 2.48$, $p = .085$, $R^2_{Adjusted} = .006$	$F(2, 492) = 4.82$, $p = .008$, $R^2_{Adjusted} = .02$	$F(2, 492) = 13.3$, $p < .001$, $R^2_{Adjusted} = .05$	$F(2, 492) = 2.60$, $p = .006$, $R^2_{Adjusted} = .08$
	-0.013649	**0.216401****	**0.068524*****	0.050215
CST	$F(2, 488) = 6.42$, $p = .002$, $R^2_{Adjusted} = .02$	$F(2, 488) = 6.19$, $p = .002$, $R^2_{Adjusted} = .02$	$F(2, 488) = 1.89$, $p = .15$, $R^2_{Adjusted} = .004$	$F(2, 488) = 1.80$, $p = .17$, $R^2_{Adjusted} = .003$
	-0.006782	0.050971	-0.018407	0.225689
ILF	$F(2, 494) = 8.03$, $p < .001$, $R^2_{Adjusted} = .03$	$F(2, 494) = 3.67$, $p = .026$, $R^2_{Adjusted} = .01$	$F(2, 494) = 2.28$, $p = .10$, $R^2_{Adjusted} = .005$	$F(2, 494) = 2.90$, $p = .06$, $R^2_{Adjusted} = .008$
	-0.019481*	-0.032828	0.004481	0.16351
SLFP	$F(2, 494) = 3.64$, $p = .027$, $R^2_{Adjusted} = .01$	$F(2, 494) = 5.51$, $p = .004$, $R^2_{Adjusted} = .02$	$F(2, 494) = 2.15$, $p = .12$, $R^2_{Adjusted} = .005$	$F(2, 494) = 4.46$, $p = .012$, $R^2_{Adjusted} = .01$
	-0.014721	**0.214620***	-0.007393	-0.247955

SLFT	$F(2, 492) = 5.01$, $p = .007$, $R^2_{Adjusted} = .02$	$F(2, 492) = 7.78$, $p = .008$, $R^2_{Adjusted} = .02$	$F(2, 492) = 4.99$, $p = .007$, $R^2_{Adjusted} = .02$	$F(2, 492) = 3.37$, $p = .035$, $R^2_{Adjusted} = .009$
	-0.021370*	**0.222030***	-0.021391	-0.127256
UNC	$F(2, 492) = 0.49$, $p = .61$, $R^2_{Adjusted} = -.002$	$F(2, 492) = 0.82$, $p = .44$, $R^2_{Adjusted} = -.0007$	$F(2, 492) = 5.06$, $p = .007$, $R^2_{Adjusted} = .02$	$F(2, 492) = 4.33$, $p = .014$, $R^2_{Adjusted} = .01$
	-0.0055602	0.1058895	0.015398	-0.143507

Table 4a: Sex differences (state-based)
Color denotes significant (p<0.05) interaction effects of sex on the association between tract order and microstructure /perfusion state were identified.
Red: higher interaction in females, Blue: higher interaction in males

	LAFO	LMFO	SPFO-MD	SMFO	ADD	VDD
FA_{perc}						
MD_{perc}						
AD_{perc}						
RD_{perc}						
CBF_{perc}						
ATT_{perc}						

Table 4b: Sex differences (rate-of-decline)
Color denotes significant (p<0.05) interaction effects of sex on the interaction of age on the association between tract order and rate of microstructure/perfusion declines were identified.
Red: higher interaction in females, Blue: higher interaction in males

	LAFO	LMFO	SPFO-MD	SMFO	ADD	VDD
FA_{perc}						
MD_{perc}						
AD_{perc}						
RD_{perc}						
CBF_{perc}						
ATT_{perc}						

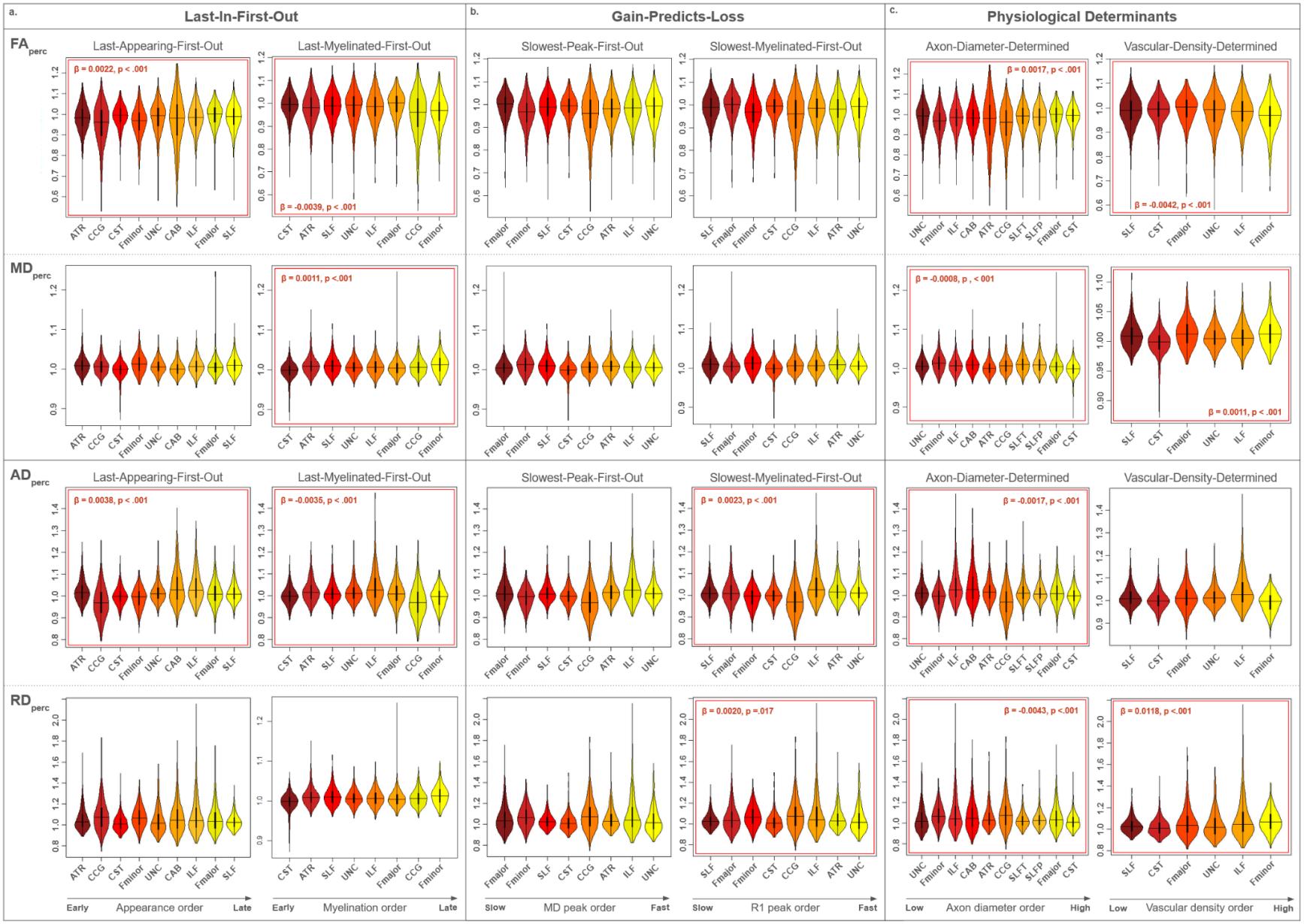
a.
Last-In-First-Out
b.
Gain-Predicts-Loss
c.
Physiological Determinants
FA perc
MD perc
AD perc
RD perc
Last-Appearing-First-Out
Last-Myelinated-First-Out
Slowest-Peak-First-Out
Slowest-Myelinated-First-Out
Axon-Diameter-Determined
Vascular-Density-Determined
β = 0.0022, p < .001
β = -0.0039, p < .001
β = 0.0017, p < .001
β = -0.0042, p < .001
β = 0.0011, p <.001
β = -0.0008, p , < 001
β = 0.0011, p < .001
β = 0.0038, p < .001
β = -0.0035, p < .001
β = 0.0023, p < .001
β = -0.0017, p < .001
β = 0.0020, p =.017
β = -0.0043, p <.001
β = 0.0118, p <.001
Early
Appearance order
Late
Myelination order
Slow
MD peak order
Fast
R1 peak order
Low
Axon diameter order
High
Vascular density order

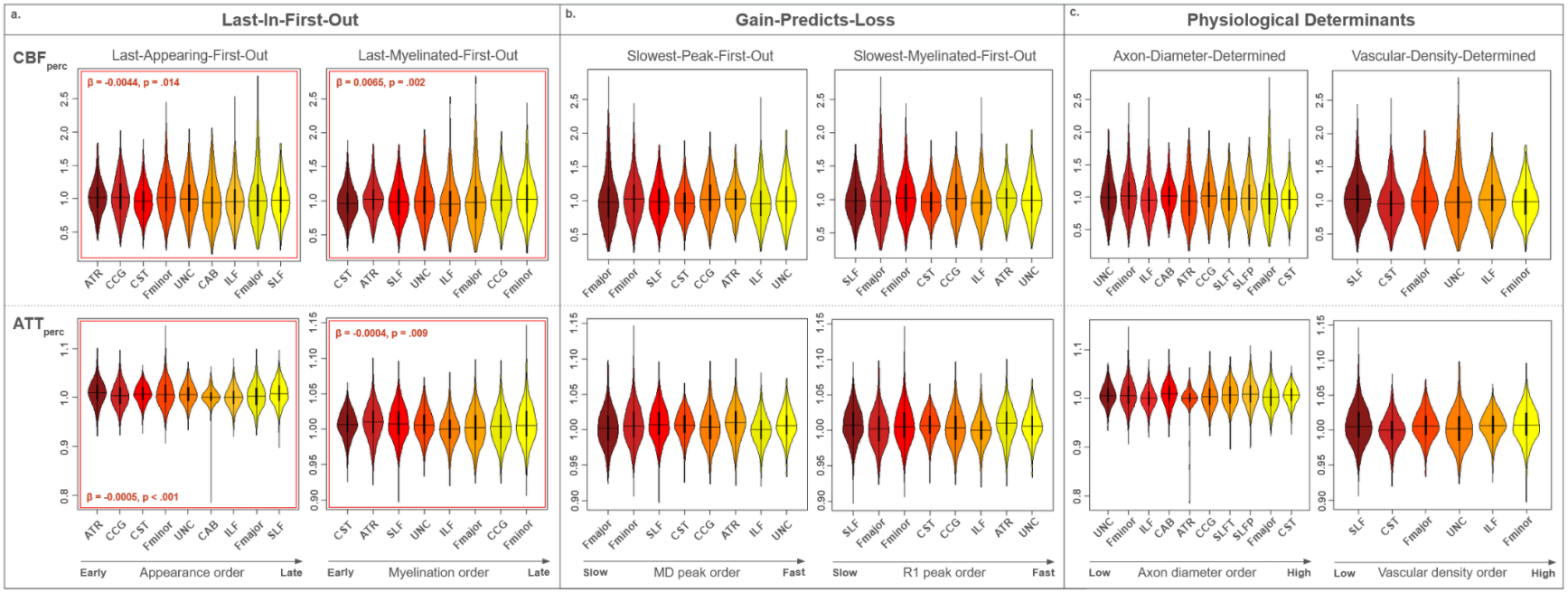

***Figure 3**: Tract-wise distributions for FA_{perc}, MD_{perc}, AD_{perc}, RD_{perc}, CBF_{perc}, and ATT_{perc} under each Last-In-First-Out (a), Gain-Predicts-Loss (b), and Physiological Determinant (c) model. Significant linear relationships between tract order and microstructural/perfusion measure are denoted with a red outline.*

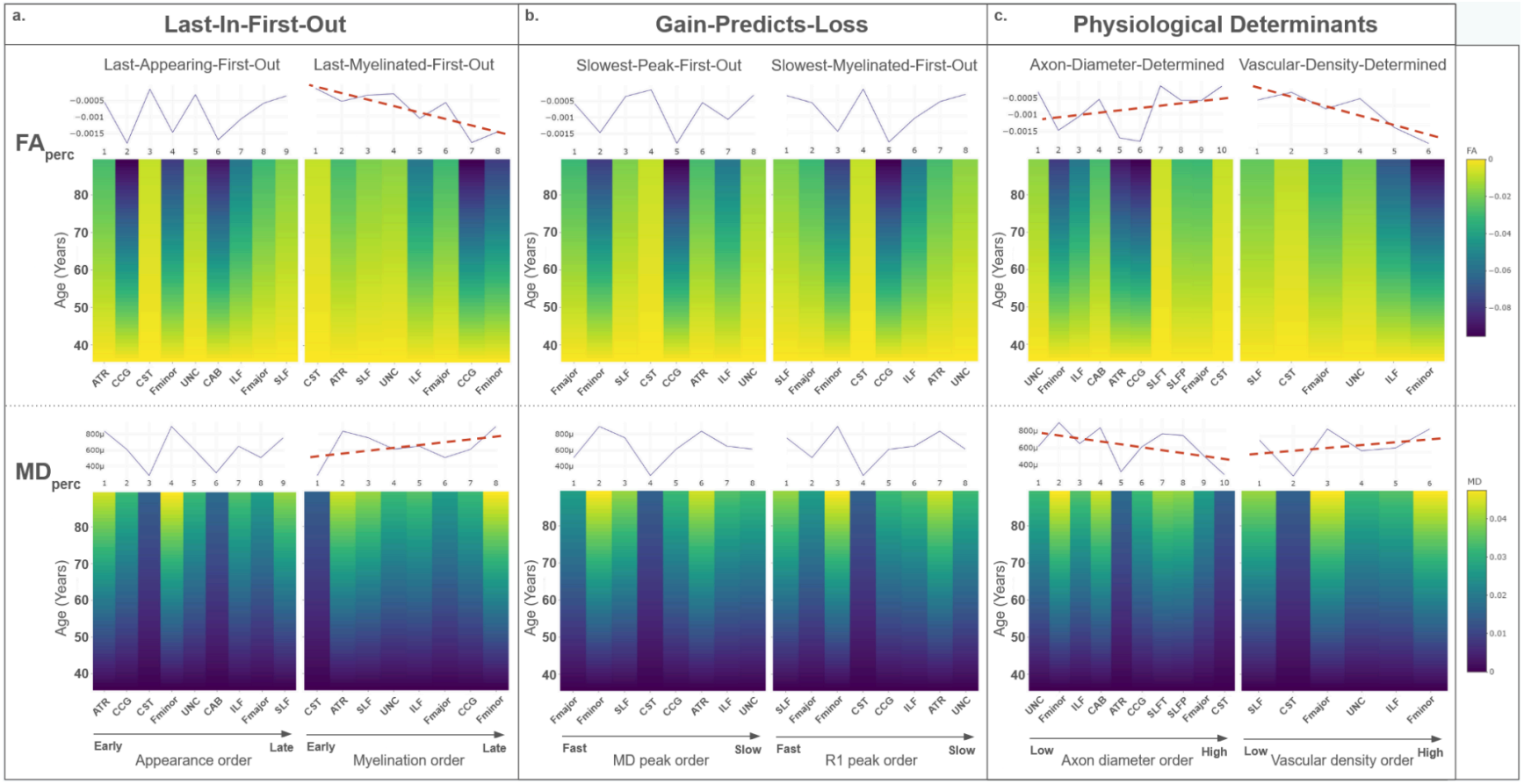
a.
Last-In-First-Out
Last-Appearing-First-Out
Last-Myelinated-First-Out
b.
Gain-Predicts-Loss
Slowest-Peak-First-Out
Slowest-Myelinated-First-Out
c.
Physiological Determinants
Axon-Diameter-Determined
Vascular-Density-Determined
FA perc
MD perc
Age (Years)
Early
Late
Appearance order
Myelination order
Fast
Slow
MD peak order
R1 peak order
Low
High
Axon diameter order
Vascular density order
FA
MD

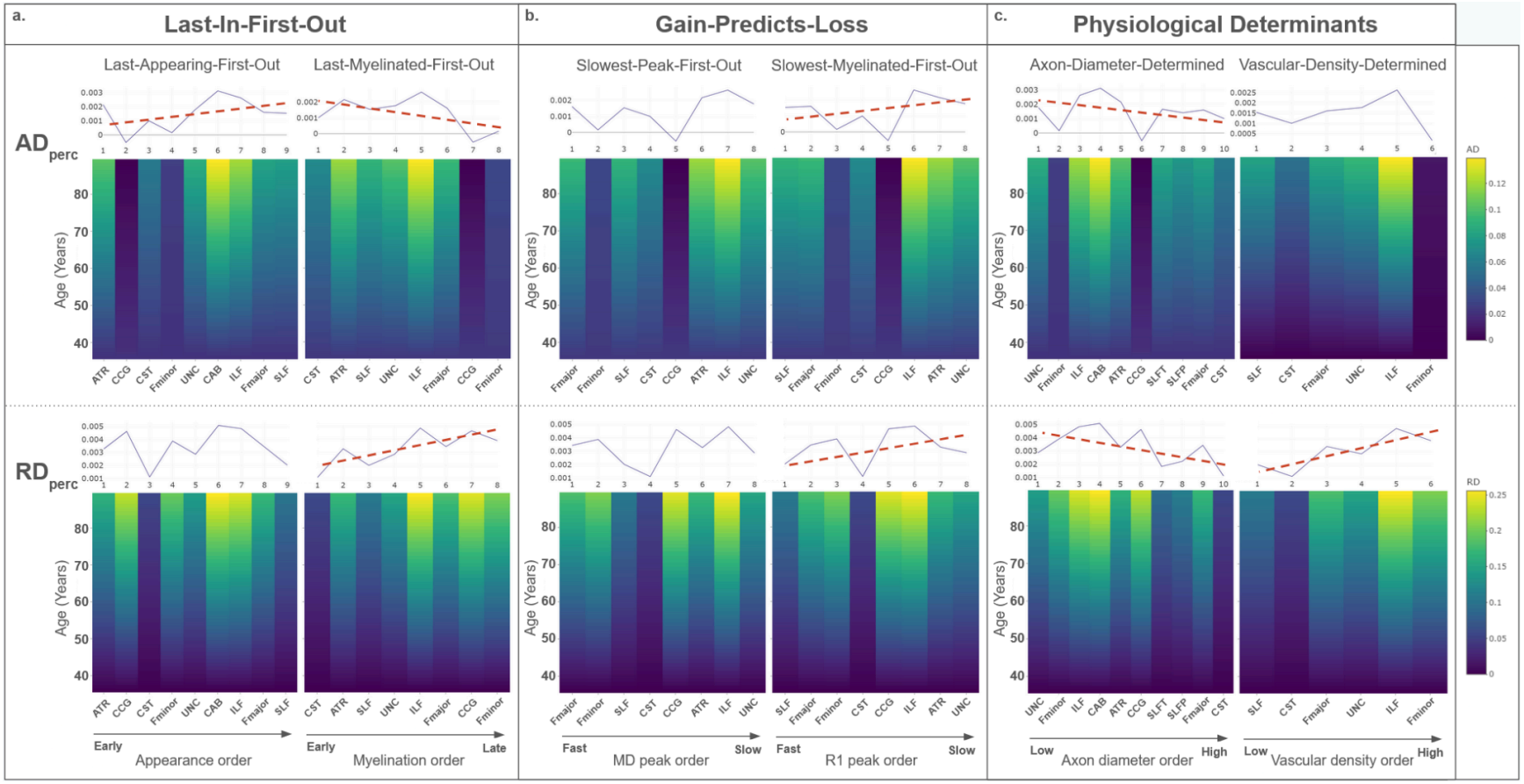
a.
Last-In-First-Out
Last-Appearing-First-Out
Last-Myelinated-First-Out
b.
Gain-Predicts-Loss
Slowest-Peak-First-Out
Slowest-Myelinated-First-Out
c.
Physiological Determinants
Axon-Diameter-Determined
Vascular-Density-Determined
AD perc
RD perc
Age (Years)
ATR CCG CST Fminor UNC CAB ILF Fmajor SLF
CST ATR SLF UNC ILF Fmajor CCG Fminor
Fmajor Fminor SLF CST CCG ATR ILF UNC
SLF Fmajor Fminor CST CCG ILF ATR UNC
UNC Fminor ILF CAB ATR CCG SLFT SLFP Fmajor CST
SLF CST Fmajor UNC ILF Fminor
Early
Appearance order
Early
Myelination order
Late
Fast
MD peak order
Slow
Fast
R1 peak order
Slow
Low
Axon diameter order
High
Low
Vascular density order
High
AD
RD

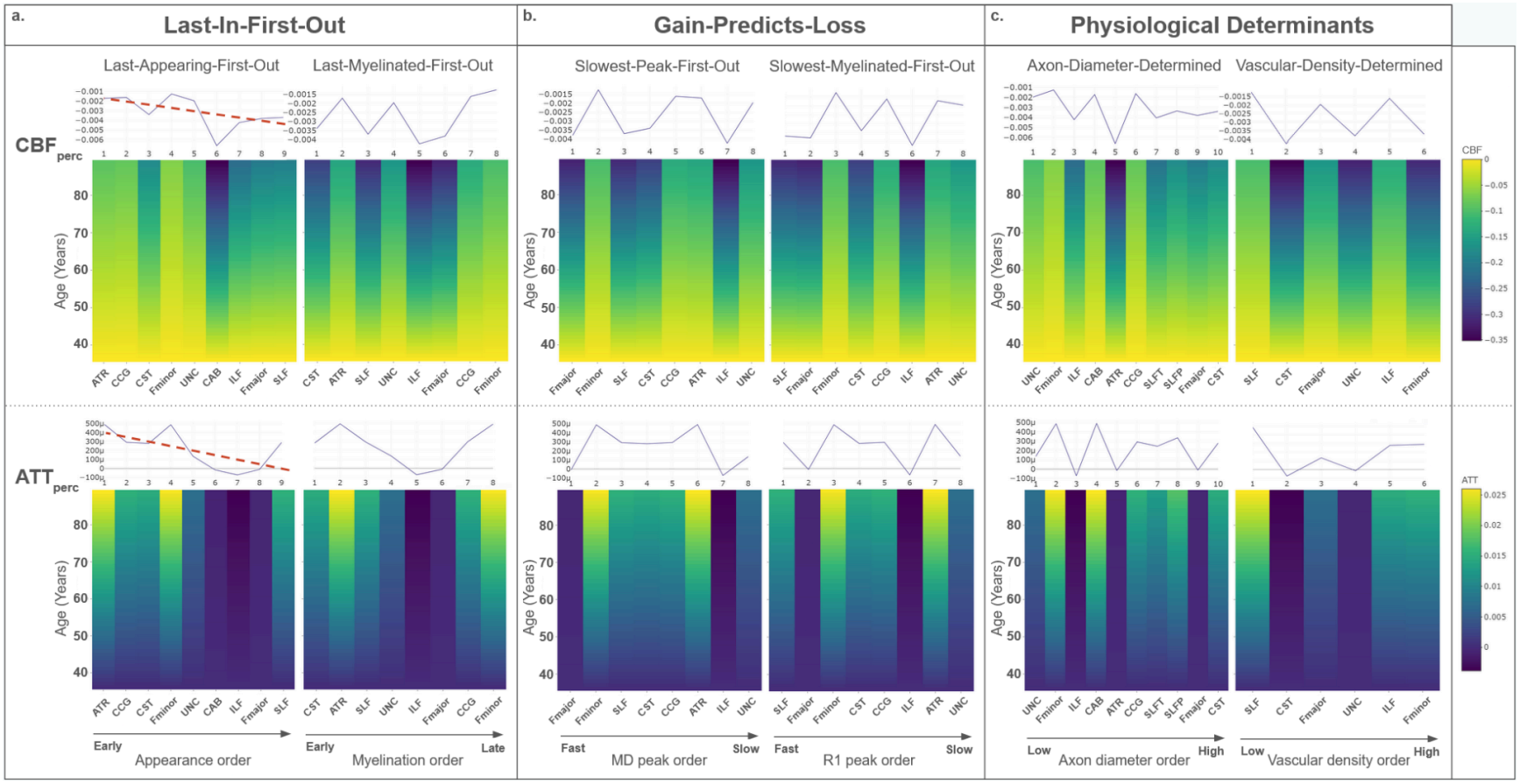

***Figure 4**: Tractwise age-effects in FA_{perc}, MDperc, AD_{perc}, RD_{perc}, CBF_{perc}, and ATT_{perc} under each Last-In-First-Out (a), Gain-Predicts-Loss (b), and Physiological Determinant (c) model. In each plot, the colours in each column indicates the values of the variable of interest modeled as a linear function of age, and bright colours represent higher values. Significant interactions between tract order and age effects on each given measure are plotted in corresponding line graphs, with dotted fit lines denoting interactions with a $p < 0.05$, with sex as a covariate.*

DISCUSSION

The retrogenesis models posed by this study hypothesized that tracts which develop earliest would show the lowest overall declines in adulthood in support of the last-in-first-out hypothesis, although "earliest developing" remains ambiguous, necessitating multiple models. Furthermore, tracts which develop most rapidly were expected to exhibit the most rapid declines in aging, in support of the gain-predicts-loss hypothesis. In comparing models, we speculated that the LMFO, and secondarily the LVFO models would represent the best fits for aging effects. While both highlighted models did demonstrate significant effects in both mean measure and age-related declines, as well as in both microstructural and perfusion measures, results gathered across the six examined models suggest a more complex relationship between tract development and degeneration than could be encapsulated by a pattern of simple ordered retrogenesis.

Order of microstructural decline

The findings of this paper shed some light on the definition of "retrogenesis", specifically in terms of (1) whether order of appearance or maturation defines "last-in"; (2) whether "last-in-first-out" or "gain-predicts-loss" better defines the retrogenesis origins.

Associations identified by the LMFO and ADD models indicate combined support for the last-in-first-out hypotheses of WM declines. Tracts with higher R1 (LMFO) and axonal diameter (ADD) at birth were associated with lower degrees of WM degeneration in terms of both FA_{perc} and MD_{perc}. As axonal diameter can be taken as a proxy for WM development, this suggests further support for a retrogenesis pattern across the tested tracts.

Conversely, the lack of significant associations between SPFO-MD and SMFO tract orders and mean FA_{perc}/MD_{perc} suggests a lack of strong support for the gain-predicts-loss hypothesis. AD/RD analysis also raised limited support for the SMFO model. While this support is limited by the lack of MD and FA significance, it can be taken as additional support for myelination as a more consistent general predictor of interest in WM declines due to the generally higher inherent sensitivity of detection by AD and RD measures in comparison to MD or FA especially when AD and RD age effects are in opposite directions. The developmental importance of myelination in building supporting connectivity and function across WM tissue (Dean et al., 2016), as well as its role in maintaining fiber integrity in aging (Davis et al., 2009), supports myelination patterns as a strong target for retrogenesis predictions.

Additionally, that ADD and LMFO models showed significant tract-order by FA_{perc}/MD_{perc} associations lends considerable support to the argument that patterns of development identified at birth,

not rates of maturation across the lifespan, predict declines in aging. Incorporating AD_{perc} and RD_{perc} into these comparisons corroborates the LMFO model's support for a retrogenesis pattern in which diffusivity becomes progressively more radial in later myelinating tracts. The understanding of retrogenesis is complicated by evidence from the LAFO model, in which the order of early prenatal tract emergence appears inversely related to adult microstructural integrity. Given that the order of tracts presented by the LAFO model follows a generally anterior to posterior pattern of tract emergence, this makes it notable as opposite to the more posterior to anterior development patterns presented by some simplified retrogenesis models (Hoagey et al., 2019; Slater et al., 2019). Across models, this seems to suggest that WM tracts myelinate in the opposite order of their initial emergence, with retrogenesis predictions supported by myelination order. However, there may be greater complexity in the trajectories of development between early prenatal development and birth that could not be captured by this study.

Regarding the link to vascular physiology, the VDD model indicates that tracts with higher macrovascular density exhibit greater susceptibility to microstructural degeneration in aging across FA_{perc}, MD_{perc} and RD_{perc} measures. This is contrary to the supposition that, like higher axonal diameter, higher macrovascular density would buffer regions against microstructural declines in aging. Instead, results from the VDD and ADD models indicate those tracts which exhibit the least aging declines have both higher axon diameter and lower macrovascular density, possibly due to lower metabolic demands by large, better insulated axon fibers (Giezendanner et al., 2016; Neishabouri & Faisal, 2011; Stassart et al., 2018).

Order of rates of microstructural decline

The rate-based analyses largely corroborated the patterns of findings shown by state-based mean microstructural analyses across our six models. That is, tracts showing greater degrees of decline also exhibit faster rates of decline in WM microstructure. Broad consistency between state-based and rate-of-decline analyses serves to emphasize support for a myelination-centric last-in-first-out hypothesis with additional influences by axon diameter and macrovascular density as shown by the LMFO, ADD, and VDD models. The only exception to this common trend is the absence of a significant interaction between tract order and age effects on FA_{perc} under the LAFO model. The limited association exhibited under the LAFO model, in which only rates of AD_{perc} declines were associated with the order of prenatal emergence, again suggests that tracts emerge in the opposite order of myelination, with earliest emerging tracts myelinating last and subsequently declining at the highest rates in aging.

The gains-predicts-loss theory is founded on rates of development and decline, raising interest in rate-of-decline analyses as potentially more representative than state-based comparisons under the gain-predicts-loss models (SMFO, SPFO-MD). However, rates of tract maturation demonstrate similarly

weak associations with rates of microstructural declines in aging across tracts. Like state-based analyses, rates of AD_{perc} and RD_{perc} were again significantly associated with tract order according to the SMFO model with no associations with tract order under the SPFO-MD model, limiting support for this interpretation of retrogenesis.

In defining "retrogenesis" with regards to microstructural declines, our results indicate that 1) patterns of development and maturation of myelination, rather than earliest appearance, better represent later declines in aging; and 2) the "last-in-first-out" model is more representative of patterns in aging declines than those predicted by "gain-predicts-loss." Our findings' support for "last-in-first-out" predictions is complicated by evidence that earliest tract appearance as modeled by the LAFO model does anticipate aging declines to some degree, however the order of appearance follows an inverse pattern best described as "last-in-last-out" that contradicts the associations proposed by retrogenesis.

Order of perfusion declines

Perfusion mostly reflects microvascular health. The LAFO model demonstrated significant associations between tract emergence order and both CBF_{perc} and ATT_{perc}. Mean CBF_{perc} was found to be highest while ATT_{perc} was longest in earliest emerging tracts. As declines in CBF are assumed to indicate a greater degree of age-related degeneration (Bernbaum et al., 2015; Chen et al., 2013), this finding would support retrogenesis in terms of perfusion decline. In contrast, increasing ATT would similarly be assumed to indicate age-related microvascular declines, which in this context would contradict the retrogenesis hypothesis. These findings demonstrate that CBF and ATT cannot be taken as synonymous measures of microvascular health. Instead, this pattern may suggest differences in regional metabolic demand or compensatory mechanisms in microvascular decline across early- and late-developing regions. That is, it is possible that early-developing regions enjoy relatively maintained overall CBF though it is delivered with an increasing ATT. With that in mind, a lengthening ATT may not always indicate impending degeneration, as age-related brain declines tend to focus on the late-developing regions, which appear to have relatively maintained ATT despite reduced CBF. This is an important finding that could alter the interpretation of ATT in the study of brain aging.

Our concurrent examination of retrogenesis effects across microstructural measures of WM health suggest the opposite pattern as that of perfusion, with varying degrees of support for greater preservation of earlier developing tracts. This distinction between microvascular and microstructural declines in the WM, along with their interactions, will require targeted examination. However, a more immediately relevant factor are the differences in developmental order indicated between models.

In contrast to the LAFO model, the LMFO model indicates that earlier myelination order in development may predict higher CBF_{perc} and with shorter ATT_{perc}, supporting the last-in-first-out

hypothesis of retrogenesis. However, as noted in microstructural comparisons by the LAFO and LMFO models, previous literature has demonstrated that the development orders in tract emergence and myelination in-utero contrast one another (Grotheer et al., 2022; Ouyang et al., 2021). Again, the question of which tract is "first-in" in terms of perfusion remains to be addressed.

Order of rates of perfusion decline

Recall that in terms of microstructural decline, results from the rate-of-decline analyses were largely consistent with those of the state-based analyses – this is not the case across models of perfusion decline. Prenatal emergence order appears to be inversely related to both state of CBF_{perc} and ATT_{perc} and rates of CBF_{perc} and ATT_{perc} change with age. That is, the earlier a tract emerges in prenatal development, the higher are the CBF_{perc} and the longer the ATT_{perc}, and the more rapidly CBF declines and ATT lengthens in aging. The co-directional association between tract order and both CBF and ATT, while counterintuitive, has been previously identified in aging haemodynamics (Yetim et al., 2023), suggesting that the "first-in-first-out" pattern found in analysis of microstructural declines is present in perfusion changes as well. The continued significance of the LAFO model for perfusion declines reinforces the assertion that prenatal emergence order represents a meaningful predictor in patterns of aging. Additional examination of early prenatal development, along with the previously suggested opposing orders of tract prenatal emergence order and tract myelination, is required to clarify how the earliest stages of prenatal development interact. Perfusion results deviate from patterns identified in microstructural declines when examining other models. The absence of predictive associations between rates of perfusion declines and tract order under the LMFO model may indicate that early prenatal emergence patterns are more strongly related to patterns of perfusion declines while patterns of myelination relate more meaningfully to microstructural declines. Limited evidence of myelination order as a predictor for perfusion declines identified under state-based analyses could be the result of more direct associations between perfusion and microstructural integrity in later age.

Microstructure-perfusion associations

Since perfusion decline may be related to tract development order, its association with microstructural decline may also follow such an order. With the majority of tracts confirming the presence of associations between microstructure and perfusion, it can be assumed that both do, to an extent, reflect a common mechanism of age-related declines. However, these associations were not universal. Associations varied by metric between tracts and three of the tracts examined (Fmajor, CST, and UNC) did not demonstrate microstructure-perfusion associations on any metric. This may suggest the presence of diverse compensatory mechanisms that support tract-wise resilience to age. For example, if a

physiological difference such as higher axon diameter were to result in a region being less metabolically demanding and thus more resilient to perfusion declines, it could prevent detection of strong associations between microvascular health and microstructural declines that are detectable in less resilient regions. While the results from this study can be taken as support for common mechanisms of declines across microstructural and perfusion measures, it is notable that microstructural and perfusion declines do not follow the same order across tracts, and are not equally predictable from the same models of retrogenesis. For example, while perfusion appears to be generally less associated with retrogenesis effects, the LAFO model's "last-in-last-out" effect was identified with both CBF_{perc} and ATT_{perc}. Further study will be necessary to elucidate the mechanism of tract-wise differences in microstructure and perfusion, particularly in the context of retrogenesis. Nonetheless, these findings undeniably support the need to study the link between developmental trajectory, microvascular health and microstructural health.

Sex-related differences

Sex differences in states of microstructural and perfusion declines across age were observed under several models, though no single pattern across all models was identified. The most prominent sex differences were found under the ADD model, whereby female subjects showed a significantly stronger association between axon diameter and both microstructural integrity (MD_{perc}, RD_{perc}) and perfusion (ATT_{perc}). These observations may suggest that either females demonstrate a greater range of axon diameters between tracts, or otherwise that females display greater differences in regional susceptibility to WM declines. While existing research on the topic remains limited, previous evidence in animal studies of corpus callosum development suggest that both of these types of sex-related differences may be present (Aboitiz et al., 1996; Pesaresi et al., 2015; Shatarat et al., 2020). Female rats demonstrate greater apparent regional differences in axonal diameter than males (Shatarat et al., 2020). Additionally, testosterone has been found to regulate axon radius, leading to higher mean axon diameter in the splenium of male than female rats (Pesaresi et al., 2015). Thus, a follow-up question related to the findings under the ADD model is whether the lower axonal diameters in females predisposes females to WM decline.

Under the SMFO model, male subjects appear to demonstrate stronger associations between microstructural decline (rising RD_{perc}) and myelination rate in early life. Additionally, under the LMFO model, males also show stronger associations between myelination order and perfusion (ATT_{perc}). Together, these findings suggest a broad trend of stronger associations between myelination and WM aging in male subjects. While myelin density is higher in males across the WM during development (Corrigan et al., 2021), neither regional g-ratio nor its aging trajectories appear to differ significantly between sexes in adulthood (Cercignani et al., 2017). Furthermore, under the LAFO model, this took the form of significantly stronger emergence-order effects on microstructural integrity (FA_{perc}) in female

subjects than males. However, under all three models, significant effects of sex were only identified in a single measure. Significant associations in a single microstructural variable such as RD_{perc} under the SMFO model may reflect differing sensitivities of different metrics. Diffusivity is inherently one of the most robust metrics of age-related decline. However, sex differences in FA_{perc} in the absence of significant AD_{perc} or RD_{perc} differences as identified under the LAFO model may suggest the presence of sex differences in crossing fiber contributions to diffusion measurements (Chad et al., 2018; Han et al., 2023). The presence of sex differences in ATT_{perc} associations in absence of CBF_{perc} differences may be related to higher blood flow velocity in female subjects more generally (Patel et al., 2016), but this association remains to be investigated in future work.

Evidence from the VDD model remains mixed, showing greater association between macrovascular density and microstructure (RD_{perc}) in male subjects despite greater association between macrovascular density and perfusion in female subjects. The contrast between these two sex differences within this model illustrates the need for a better understanding of the causal relationships between macro- and micro-vascular health as they relate to microstructural integrity in age. While sex hormones are known to be involved in the prevalence of and susceptibility to many neurovascular conditions, as well as having suggested roles in vascular autoregulation (Dion-Albert et al., 2022), differences in vascular density in the white matter remain largely understudied. Recent exploratory evidence has identified sex differences in arterial density across the brain, with female subjects showing lower values in the periventricular WM that may result in greater vulnerability to WM hypoperfusion in female subjects (Barbeau-Meunier et al., 2022).

Future directions for retrogenesis research

In addition to clarifying the stages of WM development of interest to retrogenesis as a predictive model of later aging declines, there remain gaps in our understanding of how developmental and physiological factors anticipate patterns of WM aging. The models used in this study indicate an inverse relationship between axon diameter and macrovascular density, with the additional caveat that differences in macrovascular density do not appear to correspond with differences in perfusion metrics. While the differing metabolic needs of larger versus smaller fibers may account for some of this inverse relationship, it also suggests that the relationship between axon diameter and microvascular or mesovascular, rather than macrovascular differences. The lack of relationship between WM perfusion and macrovascular density may indicate that macrovascular density is not a strong predictor of regional microvascular physiology. As such, incorporating other vascular variables into these predictive models, such as the number of regional vascular sources, may be necessary.

While between-tract differences demonstrate meaningful patterns within both this study and previous research (Robinson et al., 2023), within-tract comparisons represent an additional axis of comparisons that has received relatively little attention. Given the considerable differences in rates and patterns of development across tracts in all stages of WM growth and maturation, comparing regions within tracts along a developmental gradient may further clarify our understanding of retrogenesis as a process.

Limitations

The ordered models applied in this study are drawn from a number of prior sources examining developmental differences in the WM. As such, this examination has been limited to those studies examining similar tracts to allow for cross-model comparisons using similar reconstructed tracts. These tracts were chosen to minimize tract overlap/partial-voluming between segmentations, however, additional comparisons may be possible in more recent segmentations (Maffei et al., 2021). For instance, future work can benefit from further segmenting tracts in terms of anterior versus posterior segments.

Furthermore, as the models applied by this study are ordinal in nature due to limited availability of quantitative data on developmental differences, they remain limited in their ability to accurately represent fine differences in regional development that would be possible with quantitative models.

This study chose to address microstructural measures such as MD and FA commonly applied in existing research. This introduces limitations that may not be present with more advanced diffusion modeling.

Finally, while we have demonstrated significant relationships between tract development, physiology, and decline in this study, the cross-sectional nature of the HCP-A dataset used here could be complimented by future examinations using longitudinal data.

CONCLUSIONS

This study demonstrated support for the retrogenesis hypothesis in the form of developmental differences in myelination as a predictor for tract-wise WM microstructural and perfusion declines in aging. Also, the order of prenatal tract emergence was found to have an inverse relationship with the order of aging declines in WM, opposite that asserted by late-in-first-out predictions. Additionally, both axon diameter and macrovascular density were found to be significant physiological predictors for tract-wise aging differences, with regions of higher mean axon diameter and lower macrovascular density exhibiting higher resilience to age-related degeneration. To our knowledge, this study is the first to examine retrogenesis in the context of WM perfusion directly, and anticipate these findings will benefit ongoing understanding of the relationships between WM development and declines.

Acknowledgments

We are grateful for the financial support from the Canadian Institutes of Health Research (CIHR) (#PTJ169688) and the Canada Research Chairs (CRC) program (JJC). Research reported in this publication was supported by the National Institute On Aging of the National Institutes of Health under Award Number U01AG052564 and by funds provided by the McDonnell Center for Systems Neuroscience at Washington University in St. Louis. The HCP-Aging 2.0 Release data used in this report came from DOI: 10.15154/1520707.

REFERENCES

Aboitiz, F., Rodríguez, E., Olivares, R., & Zaidel, E. (1996). Age-related changes in fibre composition of the human corpus callosum: sex differences. *Neuroreport*, *7*(11), 1761–1764.

Arshad, M., Stanley, J. A., & Raz, N. (2016). Adult age differences in subcortical myelin content are consistent with protracted myelination and unrelated to diffusion tensor imaging indices. *NeuroImage*, *143*, 26–39.

Barbeau-Meunier, C.-A., Bernier, M., Côté, S., Gilbert, G., Bocti, C., & Whittingstall, K. (2022). Sexual dimorphism in the cerebrovascular network: Brain MRI shows lower arterial density in women. *Journal of Neuroimaging: Official Journal of the American Society of Neuroimaging*, *32*(2), 337–344.

Bernbaum, M., Menon, B. K., Fick, G., Smith, E. E., Goyal, M., Frayne, R., & Coutts, S. B. (2015). Reduced blood flow in normal white matter predicts development of leukoaraiosis. *Journal of Cerebral Blood Flow and Metabolism: Official Journal of the International Society of Cerebral Blood Flow and Metabolism*, *35*(10), 1610–1615.

Bernier, M., Viessmann, O., Ohringer, N., Chen, J. E., Fultz, N. E., Leaf, R. K., Wald, L. L., & Polimeni, J. R. (2020). Human cerebral white-matter vasculature imaged using the blood-Pool contrast agent ferumoxytol: bundle-specific vessels and vascular density. *Proc Intl Soc Mag Reson Med*, *28*, 0016.

Bookheimer, S. Y., Salat, D. H., Terpstra, M., Ances, B. M., Barch, D. M., Buckner, R. L., Burgess, G. C., Curtiss, S. W., Diaz-Santos, M., Elam, J. S., Fischl, B., Greve, D. N., Hagy, H. A., Harms, M. P., Hatch, O. M., Hedden, T., Hodge, C., Japardi, K. C., Kuhn, T. P., … Yacoub, E. (2019). The Lifespan Human Connectome Project in Aging: An overview. *NeuroImage*, *185*, 335–348.

Brody, B. A., Kinney, H. C., Kloman, A. S., & Gilles, F. H. (1987). Sequence of central nervous system myelination in human infancy. I. An autopsy study of myelination. *Journal of Neuropathology and Experimental Neurology*, *46*(3), 283–301.

Cercignani, M., Giulietti, G., Dowell, N. G., Gabel, M., Broad, R., Leigh, P. N., Harrison, N. A., &

Bozzali, M. (2017). Characterizing axonal myelination within the healthy population: a tract-by-tract mapping of effects of age and gender on the fiber g-ratio. *Neurobiology of Aging*, *49*, 109–118.

Chad, J. A., Pasternak, O., Salat, D. H., & Chen, J. J. (2018). Re-examining age-related differences in white matter microstructure with free-water corrected diffusion tensor imaging. *Neurobiology of Aging*, *71*, 161–170.

Chappell, M. A., Groves, A. R., MacIntosh, B. J., Donahue, M. J., Jezzard, P., & Woolrich, M. W. (2011). Partial volume correction of multiple inversion time arterial spin labeling MRI data. *Magnetic Resonance in Medicine: Official Journal of the Society of Magnetic Resonance in Medicine / Society of Magnetic Resonance in Medicine*, *65*(4), 1173–1183.

Chappell, M. A., Groves, A. R., Whitcher, B., & Woolrich, M. W. (2009). Variational Bayesian Inference for a Nonlinear Forward Model. *IEEE Transactions on Signal Processing: A Publication of the IEEE Signal Processing Society*, *57*(1), 223–236.

Chen, J. J., Rosas, H. D., & Salat, D. H. (2013). The relationship between cortical blood flow and sub-cortical white-matter health across the adult age span. *PloS One*, *8*(2), e56733.

Corrigan, N. M., Yarnykh, V. L., Hippe, D. S., Owen, J. P., Huber, E., Zhao, T. C., & Kuhl, P. K. (2021). Myelin development in cerebral gray and white matter during adolescence and late childhood. *NeuroImage*, *227*, 117678.

Cox, S. R., Ritchie, S. J., Tucker-Drob, E. M., Liewald, D. C., Hagenaars, S. P., Davies, G., Wardlaw, J. M., Gale, C. R., Bastin, M. E., & Deary, I. J. (2016). Ageing and brain white matter structure in 3,513 UK Biobank participants. *Nature Communications*, *7*, 13629.

Davis, S. W., Dennis, N. A., Buchler, N. G., White, L. E., Madden, D. J., & Cabeza, R. (2009). Assessing the effects of age on long white matter tracts using diffusion tensor tractography. *NeuroImage*, *46*(2), 530–541.

Dean, D. C., 3rd, O'Muircheartaigh, J., Dirks, H., Travers, B. G., Adluru, N., Alexander, A. L., & Deoni, S. C. L. (2016). Mapping an index of the myelin g-ratio in infants using magnetic resonance imaging. *NeuroImage*, *132*, 225–237.

de Groot, M., Cremers, L. G. M., Ikram, M. A., Hofman, A., Krestin, G. P., van der Lugt, A., Niessen, W. J., & Vernooij, M. W. (2016). White Matter Degeneration with Aging: Longitudinal Diffusion MR Imaging Analysis. *Radiology*, *279*(2), 532–541.

Dion-Albert, L., Bandeira Binder, L., Daigle, B., Hong-Minh, A., Lebel, M., & Menard, C. (2022). Sex differences in the blood-brain barrier: Implications for mental health. *Frontiers in Neuroendocrinology*, *65*, 100989.

Genc, S., Smith, R. E., Malpas, C. B., Anderson, V., Nicholson, J. M., Efron, D., Sciberras, E., Seal, M. L., & Silk, T. J. (2018). Development of white matter fibre density and morphology over childhood: A longitudinal fixel-based analysis. *NeuroImage*, *183*, 666–676.

Giezendanner, S., Fisler, M. S., Soravia, L. M., Andreotti, J., Walther, S., Wiest, R., Dierks, T., & Federspiel, A. (2016). Microstructure and Cerebral Blood Flow within White Matter of the Human Brain: A TBSS Analysis. *PloS One*, *11*(3), e0150657.

Grotheer, M., Rosenke, M., Wu, H., Kular, H., Querdasi, F. R., Natu, V. S., Yeatman, J. D., & Grill-Spector, K. (2022). White matter myelination during early infancy is linked to spatial gradients and myelin content at birth. *Nature Communications*, *13*(1), 997.

Han, A., Dhollander, T., Sun, Y. L., Chad, J. A., & Chen, J. J. (2023). Fiber-specific age-related differences in the white matter of healthy adults uncovered by fixel-based analysis. *Neurobiology of Aging*, *130*, 22–29.

Harms, M. P., Somerville, L. H., Ances, B. M., Andersson, J., Barch, D. M., Bastiani, M., Bookheimer, S. Y., Brown, T. B., Buckner, R. L., Burgess, G. C., Coalson, T. S., Chappell, M. A., Dapretto, M., Douaud, G., Fischl, B., Glasser, M. F., Greve, D. N., Hodge, C., Jamison, K. W., … Yacoub, E. (2018). Extending the Human Connectome Project across ages: Imaging protocols for the Lifespan Development and Aging projects. *NeuroImage*, *183*, 972–984.

Hoagey, D. A., Rieck, J. R., Rodrigue, K. M., & Kennedy, K. M. (2019). Joint contributions of cortical morphometry and white matter microstructure in healthy brain aging: A partial least squares correlation analysis. *Human Brain Mapping*, *40*(18), 5315–5329.

Huang, H., Xue, R., Zhang, J., Ren, T., Richards, L. J., Yarowsky, P., Miller, M. I., & Mori, S. (2009). Anatomical characterization of human fetal brain development with diffusion tensor magnetic resonance imaging. *The Journal of Neuroscience: The Official Journal of the Society for Neuroscience*, *29*(13), 4263–4273.

Huang, H., Zhang, J., Wakana, S., Zhang, W., Ren, T., Richards, L. J., Yarowsky, P., Donohue, P., Graham, E., van Zijl, P. C. M., & Mori, S. (2006). White and gray matter development in human fetal, newborn and pediatric brains. *NeuroImage*, *33*(1), 27–38.

Huang, S. Y., Tian, Q., Fan, Q., Witzel, T., Wichtmann, B., McNab, J. A., Daniel Bireley, J., Machado, N., Klawiter, E. C., Mekkaoui, C., Wald, L. L., & Nummenmaa, A. (2020). High-gradient diffusion MRI reveals distinct estimates of axon diameter index within different white matter tracts in the in vivo human brain. *Brain Structure & Function*, *225*(4), 1277–1291.

Kiely, M., Triebswetter, C., Cortina, L. E., Gong, Z., Alsameen, M. H., Spencer, R. G., & Bouhrara, M. (2022). Insights into human cerebral white matter maturation and degeneration across the adult lifespan. *NeuroImage*, *247*, 118727.

Lebel, C., & Beaulieu, C. (2011). Longitudinal development of human brain wiring continues from childhood into adulthood. *The Journal of Neuroscience: The Official Journal of the Society for Neuroscience*, *31*(30), 10937–10947.

Maffei, C., Lee, C., Planich, M., Ramprasad, M., Ravi, N., Trainor, D., Urban, Z., Kim, M., Jones, R. J., Henin, A., Hofmann, S. G., Pizzagalli, D. A., Auerbach, R. P., Gabrieli, J. D. E., Whitfield-Gabrieli, S., Greve, D. N., Haber, S. N., & Yendiki, A. (2021). Using diffusion MRI data acquired with ultra-high gradients to improve tractography in routine-quality data. In *bioRxiv* (p. 2021.06.28.450265). https://doi.org/10.1101/2021.06.28.450265

Michielse, S., Coupland, N., Camicioli, R., Carter, R., Seres, P., Sabino, J., & Malykhin, N. (2010). Selective effects of aging on brain white matter microstructure: a diffusion tensor imaging tractography study. *NeuroImage*, *52*(4), 1190–1201.

Neishabouri, A. M., & Faisal, A. A. (2011). The metabolic efficiency of myelinated vs unmyelinated

axons. *BMC Neuroscience*, *12*(1), 1–2.

Ouyang, Y., Cui, D., Yuan, Z., Liu, Z., Jiao, Q., Yin, T., & Qiu, J. (2021). Analysis of Age-Related White Matter Microstructures Based on Diffusion Tensor Imaging. *Frontiers in Aging Neuroscience*, *13*, 664911.

Patel, N., Panerai, R. B., Haunton, V., Katsogridakis, E., Saeed, N. P., Salinet, A., Brodie, F., Syed, N., D'Sa, S., & Robinson, T. G. (2016). The Leicester cerebral haemodynamics database: normative values and the influence of age and sex. *Physiological Measurement*, *37*(9), 1485–1498.

Pesaresi, M., Soon-Shiong, R., French, L., Kaplan, D. R., Miller, F. D., & Paus, T. (2015). Axon diameter and axonal transport: In vivo and in vitro effects of androgens. *NeuroImage*, *115*, 191–201.

Robinson, T. D., Sun, Y. L., Chang, P. T. H., & Jean Chen, J. (2023). In search of a unifying theory of white matter aging: associations with age in perfusion detectable in advance of microstructure. In *bioRxiv* (p. 2023.06.30.547294). https://doi.org/10.1101/2023.06.30.547294

Schilling, K. G., Archer, D., Yeh, F.-C., Rheault, F., Cai, L. Y., Hansen, C., Yang, Q., Ramdass, K., Shafer, A. T., Resnick, S. M., Pechman, K. R., Gifford, K. A., Hohman, T. J., Jefferson, A., Anderson, A. W., Kang, H., & Landman, B. A. (2022). Aging and white matter microstructure and macrostructure: a longitudinal multi-site diffusion MRI study of 1218 participants. *Brain Structure & Function*, *227*(6), 2111–2125.

Shatarat, A., Alzghoul, L., Al-Qattan, D., & ELBeltagy, M. (2020). Anatomical and ultrastructural sex differences in mean diameter and thickness of myelinated axons in adult rat corpus callosum. *International Journal of Morphology = Revista Internacional de Morfologia*, *38*(2), 505–512.

Slater, D. A., Melie-Garcia, L., Preisig, M., Kherif, F., Lutti, A., & Draganski, B. (2019). Evolution of white matter tract microstructure across the life span. *Human Brain Mapping*, *40*(7), 2252–2268.

Stassart, R. M., Möbius, W., Nave, K.-A., & Edgar, J. M. (2018). The Axon-Myelin Unit in Development and Degenerative Disease. *Frontiers in Neuroscience*, *12*, 467.

Stricker, N. H., Schweinsburg, B. C., Delano-Wood, L., Wierenga, C. E., Bangen, K. J., Haaland, K. Y., Frank, L. R., Salmon, D. P., & Bondi, M. W. (2009). Decreased white matter integrity in

late-myelinating fiber pathways in Alzheimer's disease supports retrogenesis. *NeuroImage*, *45*(1), 10–16.

Yeatman, J. D., Wandell, B. A., & Mezer, A. A. (2014). Lifespan maturation and degeneration of human brain white matter. *Nature Communications*, *5*, 4932.

Yendiki, A., Panneck, P., Srinivasan, P., Stevens, A., Zöllei, L., Augustinack, J., Wang, R., Salat, D., Ehrlich, S., Behrens, T., Jbabdi, S., Gollub, R., & Fischl, B. (2011). Automated probabilistic reconstruction of white-matter pathways in health and disease using an atlas of the underlying anatomy. *Frontiers in Neuroinformatics*, *5*, 23.

Yetim, E., Jacoby, J., Damestani, N. L., Lovely, A. E., Salat, D. H., & Juttukonda, M. R. (2023). Mean arterial pressure and cerebral hemodynamics across the lifespan: A cross-sectional study from Human Connectome Project-aging. *Journal of Magnetic Resonance Imaging: JMRI*, *58*(6), 1892–1900.

Yu, Q., Peng, Y., Kang, H., Peng, Q., Ouyang, M., Slinger, M., Hu, D., Shou, H., Fang, F., & Huang, H. (2020). Differential White Matter Maturation from Birth to 8 Years of Age. *Cerebral Cortex* , *30*(4), 2673–2689.